Cell Reports, Volume *42*

Supplemental information

NK cells propagate T cell immunity following *in situ* tumor vaccination

Won Jong Jin, Justin C. Jagodinsky, Jessica M. Vera, Paul A. Clark, Cindy L. Zuleger, Amy K. Erbe, Irene M. Ong, Trang Le, Kaitlin Tetreault, Tracy Berg, Alexander L. Rakhmilevich, KyungMann Kim, Michael A. Newton, Mark R. Albertini, Paul M. Sondel, and Zachary S. Morris

Supplementary figure 1

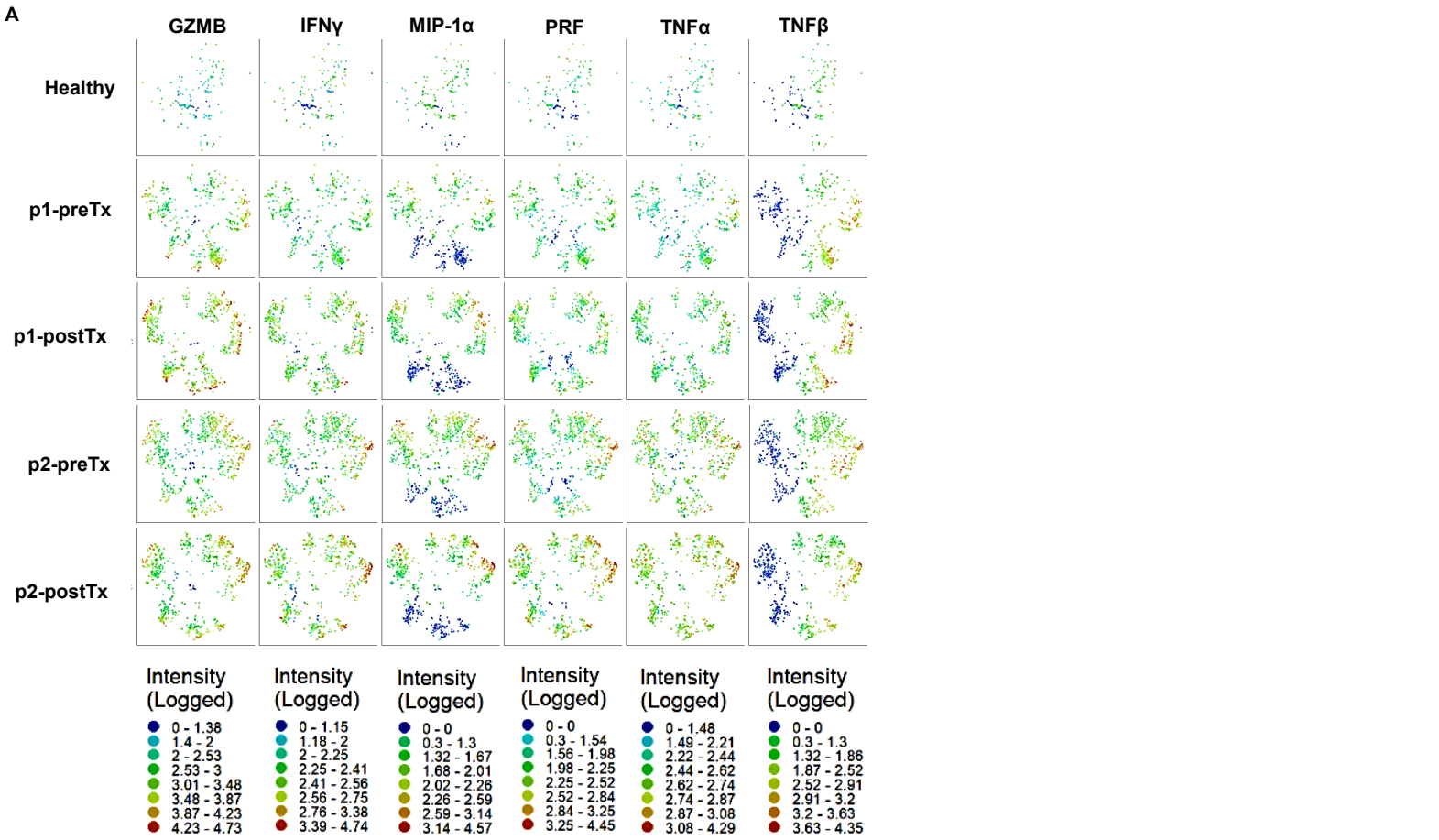

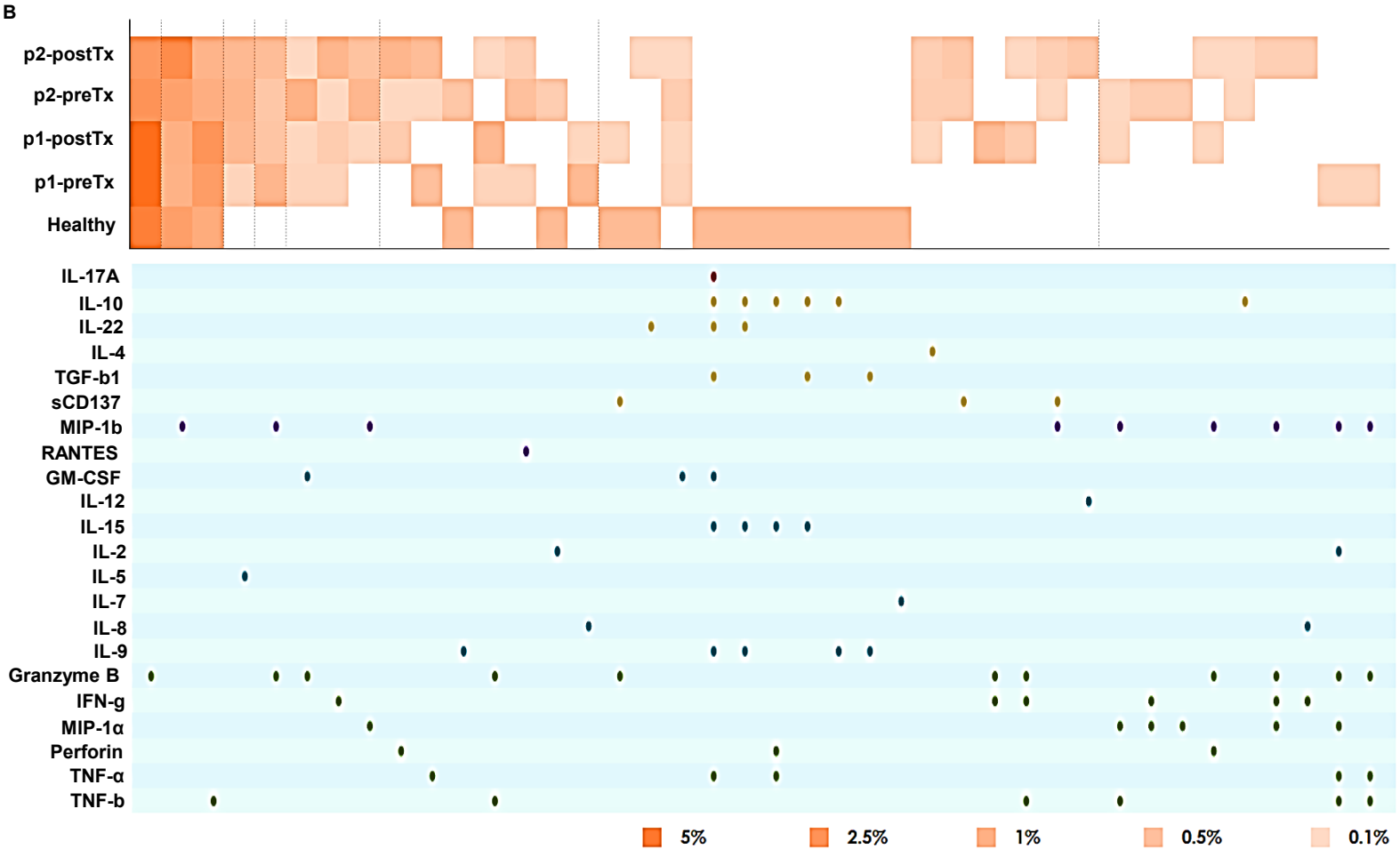

Supplementary figure 1

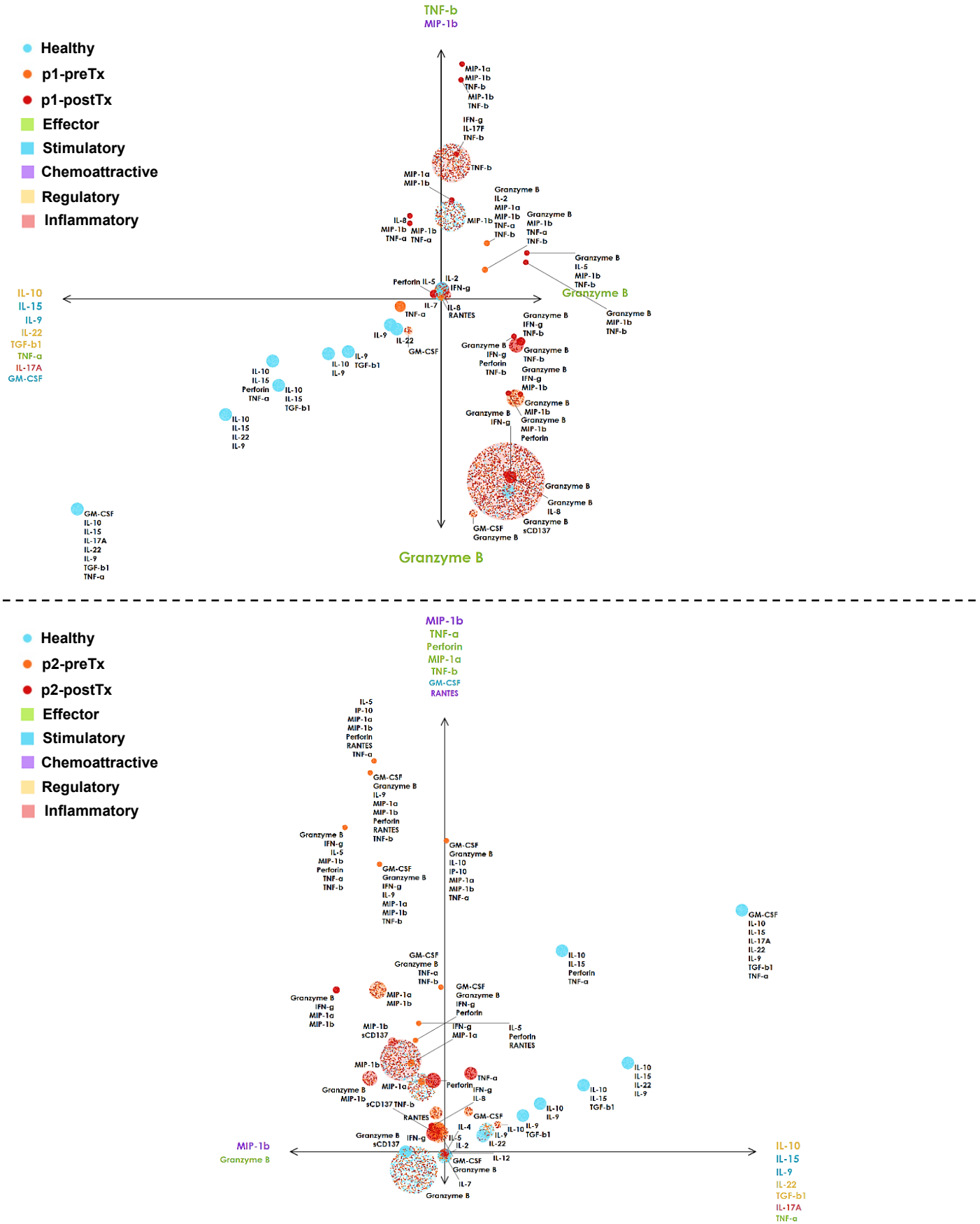

Figure S1. In situ vaccination with tumor-directed radiation and intratumoral hu14.18-IL2 induces a polyfunctional CD8+ T cell response in patients with melanoma (Related to Figure 1)

(A) 2D t-SNE visualization of single-cell effector protein signal intensity.

(B) Polyfunctional heatmap.

(C) Polyfunctional activation topology PCA plot. Broad circles indicate each cytokine group; small dots indicate a single cell data point. Circle size corresponds to how frequently the samples secreted the cytokine group.

Supplementary figure 2

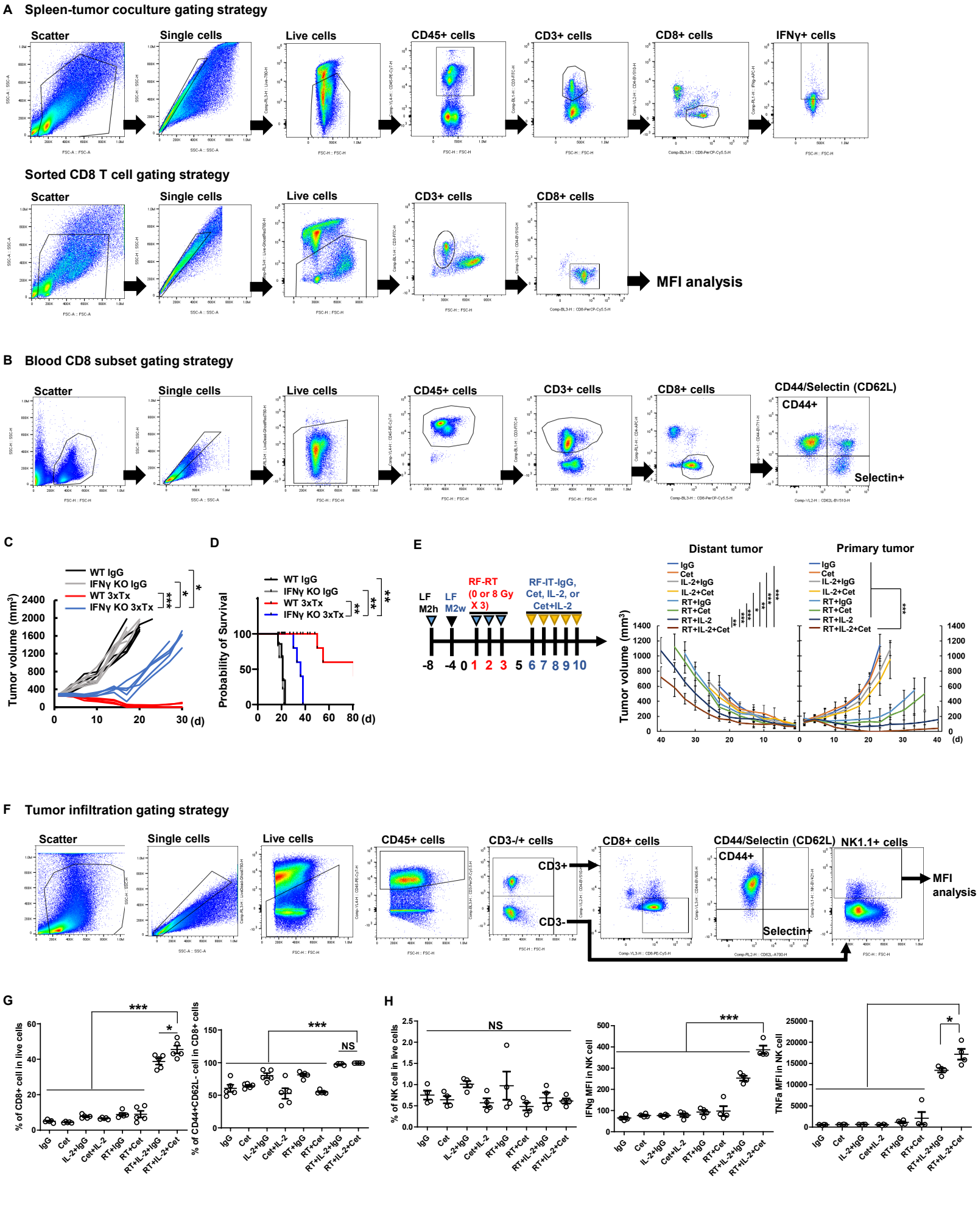

Supplementary figure 2

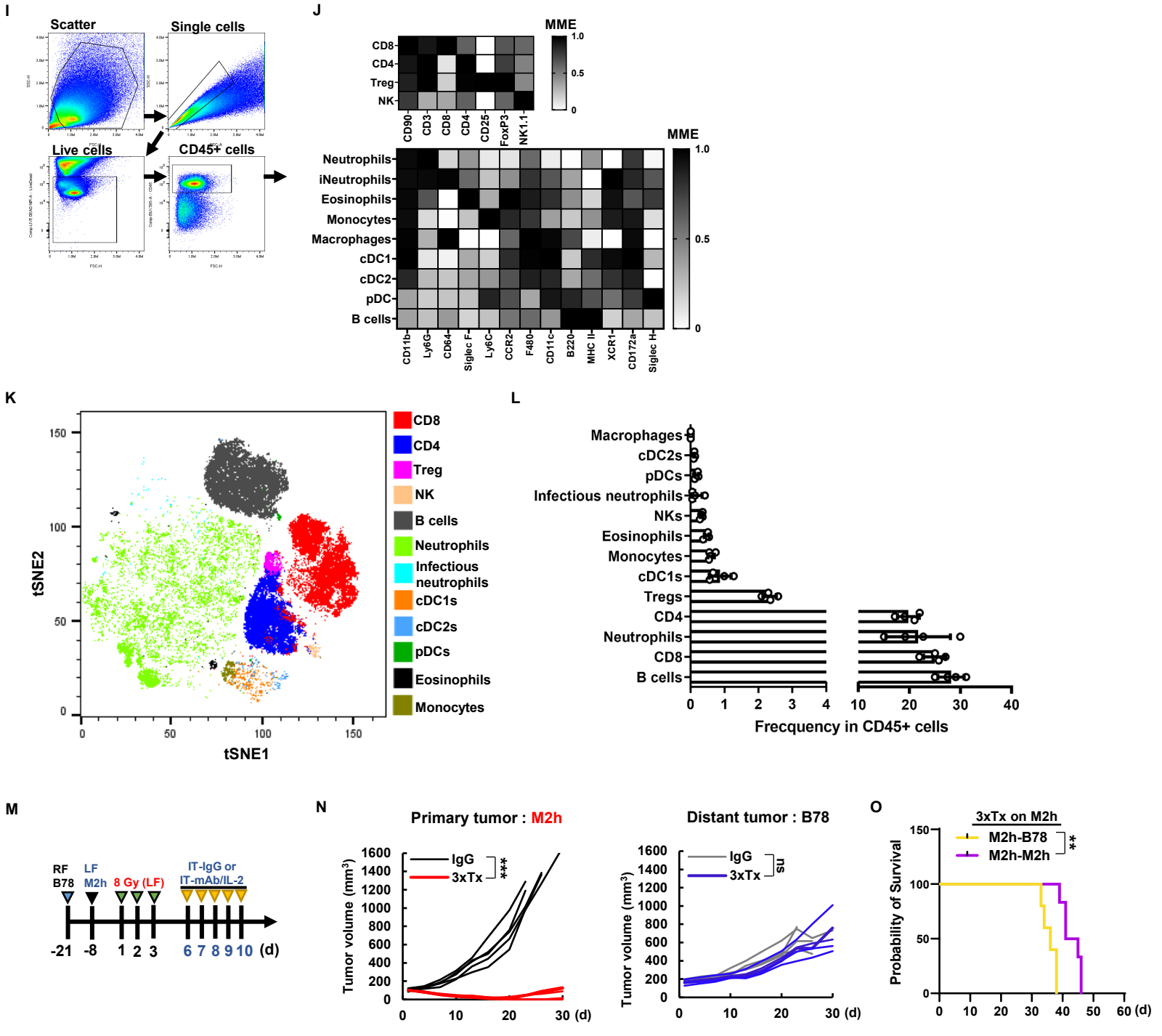

Figure S2. Local 3xTx induces tumor-specific CD8+ T cell immunity (Related to Figure 3)

(A and B) Gating strategy of flow cytometry.

(C) Individual tumor volume and (D) survival data. (n = 5)

E-H. Bilateral tumor-bearing mice received IgG, cetuximab (Cet), IL-2, or/and RT on the primary tumor (RF-right flank).

(E) Treatment regimen (left) and mean tumor volume (right). (n = 6-8)

(F) Gating strategy of flow cytometry.

(G) Analysis of $CD8^+$ cell infiltration (left) and T_{cm} ($Selectin^-CD44^+$) of $CD8^+$ T cells. (n = 5)

(H) Analysis of NK1.1+ cell infiltration (left), IFNγ MFI (middle), and TNFα MFI (right). (n = 5)

I-L, Bilateral tumor-bearing mice (RF-M2h and LF-M2w) received 3xTx on the RF and RF tumors collected on d12.

(I) Gating strategy of spectral flow cytometry for $Live^+CD45^+$ cells.

(J) Immune cell classification heatmap based on the Flowsom-derived median marker expression (MME).

(K) tSNE plot of CD45-positive compartment.

(L) Analysis of $CD45^+$ immune compartment. (n = 4)

M-O, Bilateral tumor bearing mice (RF-B78 and LF-M2h) received IgG or 3xTx on the LF-M2h.

(M) Treatment regimen, (N) individual tumor volume, and (O) survival data. (n = 5-6)

Data represent the mean ± SD. ns, not significant; $*P \leq 0.05$; $**P \leq 0.01$; $***P \leq 0.001$.

Supplementary figure 3

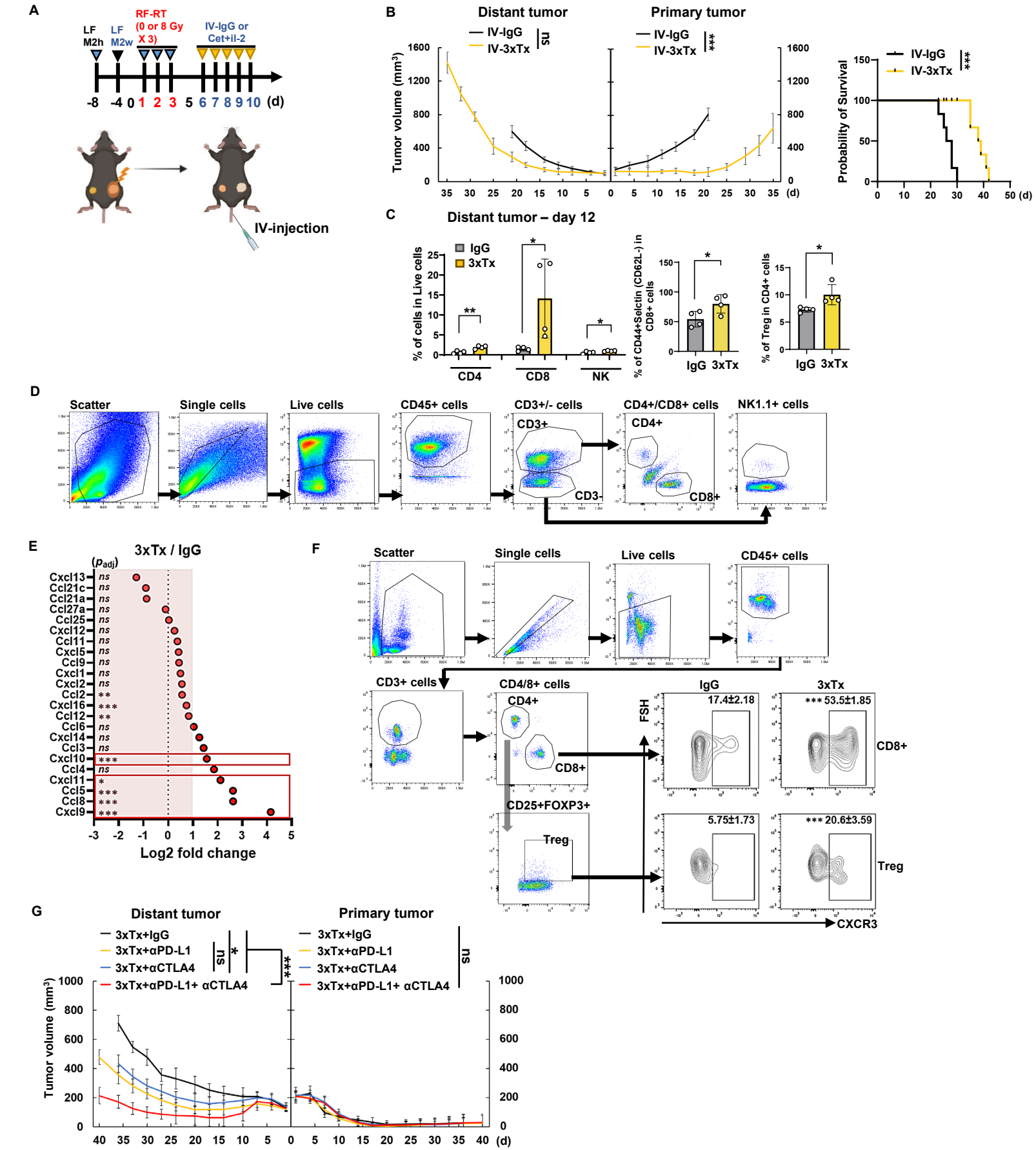

Figure S3. 3xTx induces chemokine expression in the distant tumor and CXCR3 expression in circulating CD8+ T cells and Treg (Related to Figure 4)

A-C, Bilateral tumor-bearing mice (RF-M2h and LF-M2w) received IgG intravenously (IV-IgG) or RF-radiation, cetuximab and IL-2 intravenously (IV-3xTx).

(A) Treatment regimen.

(B) Mean tumor volume (left) and survival data (right). (n = 5)

(C) Analysis of immune cells infiltration in the distant tumor. (n = 4)

(D) Gating strategy.

(E) Analysis of chemokine gene expression in the distant tumor pooled from RNA-seq analysis. padj, adjusted p-value.

(F) Gating strategy and CXCR3-expressing cell in $CD8^+$ T cell or Treg ($CD4^+CD25^+FOXP3^+$). (n = 4)

(G) Mean tumor volume from anti-PDL1 and/or anti-CTLA4 antibody treated mice. (n = 8)

All data represent the mean ± SD. ns, not significant; *P ≤ 0.05; **P ≤ 0.01; ***P ≤ 0.001.

Supplementary figure 4

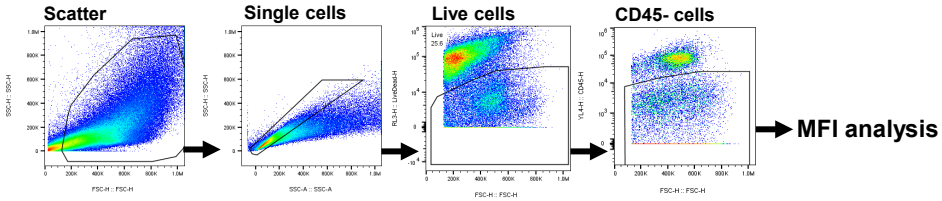

Figure S4. The gating strategy of flow cytometry **(Related to Figure 5)**

Supplementary figure 5

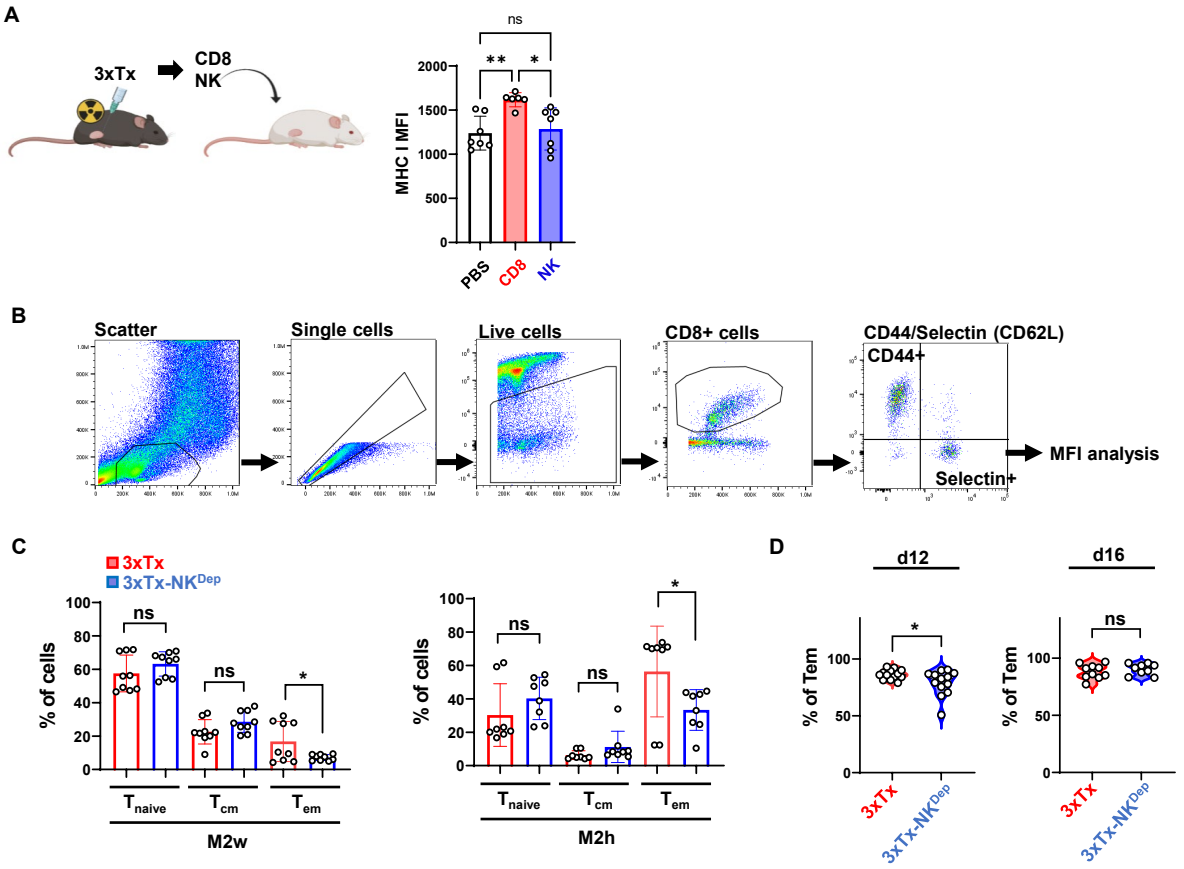

Figure S5. Depletion of NK cells reduces CD8$^+$ T cell polyfunctionality (Related to Figure 6)

(A) Bilateral tumor-bearing mice (RF-M2h and LF-M2w) received 3xTx on the RF. On d12, CD8$^+$ T cells or NK cells sorted from the mouse spleens were intratumorally injected in M2w-bearing immunodeficient NSG mice (left). Analysis of MHC I MFI in live$^+$CD45$^-$ cells (right).
B and C, Bilateral tumor-bearing mice (RF-M2h and LF-M2w) received 3xTx on the RF. During treatment, IgG (3xTx) or anti-NK1.1 antibody (3xTx-NK^{dep}) was injected intraperitoneally. On d22, CD8$^+$ T cells sorted from spleens were co-cultured with pre-plated M2w or M2h for 5 days.
(B) Gating strategy.
(C) Analysis of CD8$^+$ subset. (n = 8-9)
(D) Analysis of T_{cm} of CD8$^+$ T cells in the distant tumor. (n = 9-13)
Data represent the mean ± SD. ns, not significant; *P ≤ 0.05; **P ≤ 0.01.

Supplementary figure 6

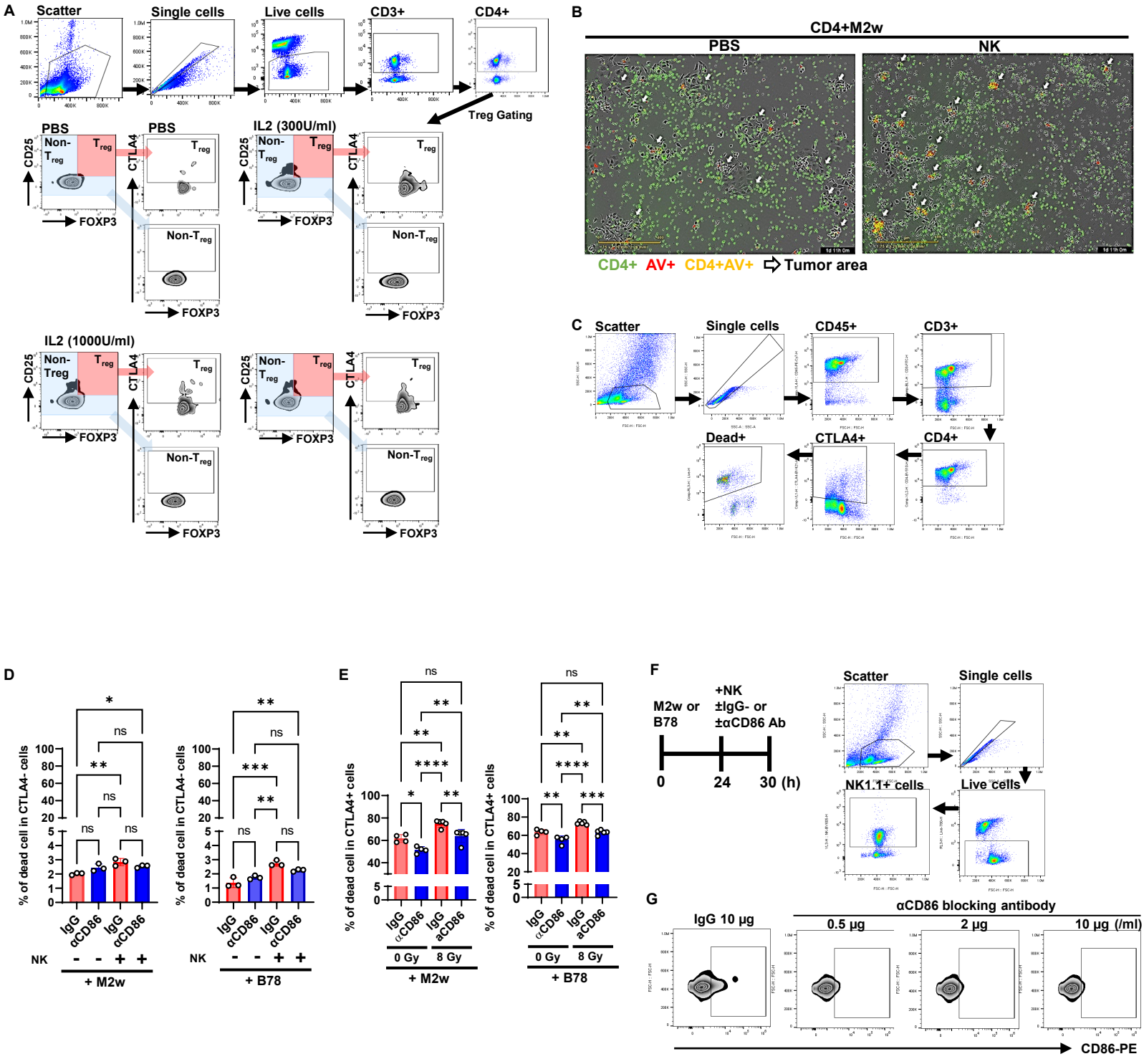

Supplementary figure 6

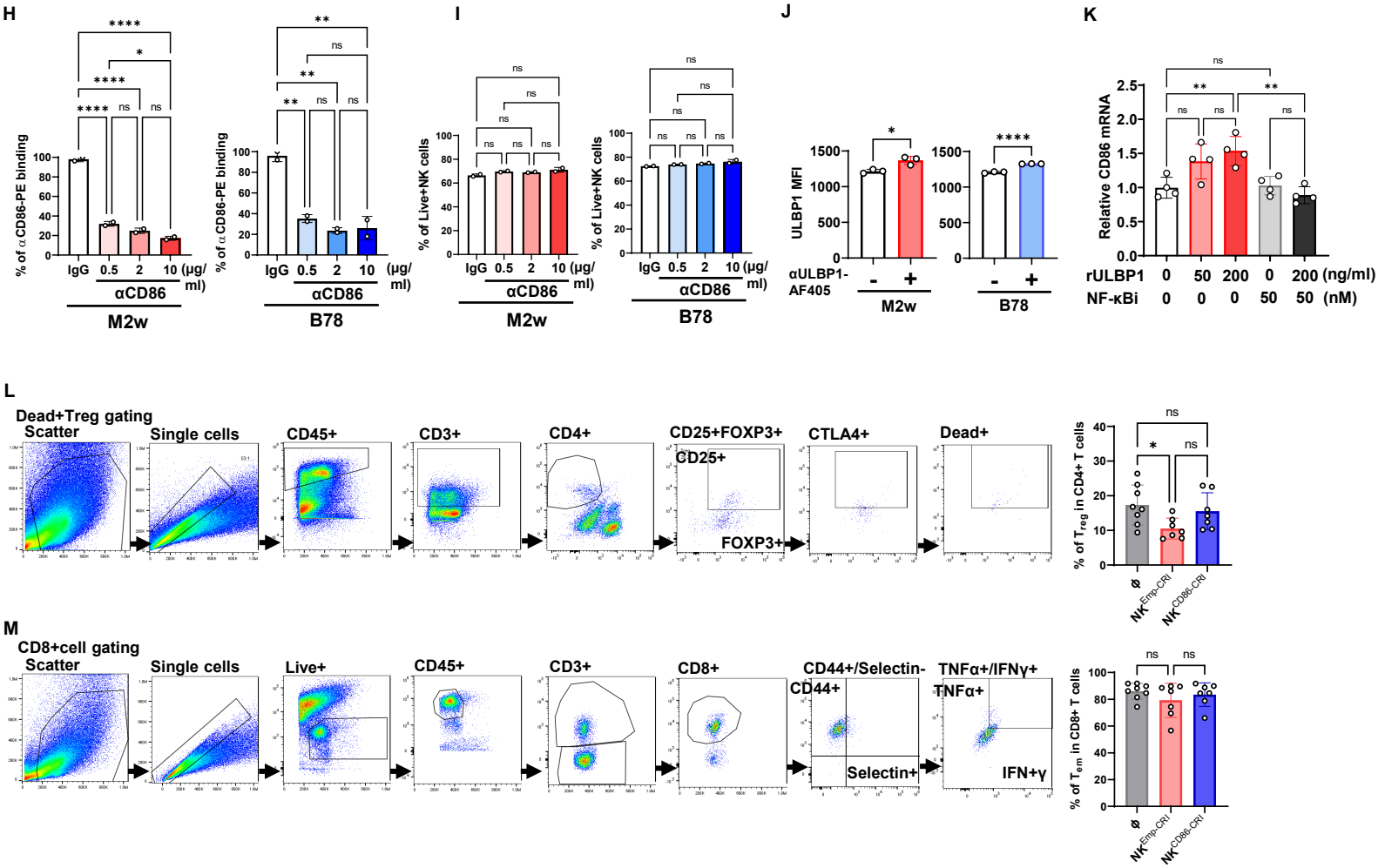

Figure S6. NK cells antagonize CTLA4$^+$ Treg via KLRK1-CD86 axis (Related to Figure 7)

(A) Analysis of IL2-mediated CTLA4 expression in Treg (CD4$^+$CD25$^+$FOXP3$^+$)

(B) Detection of annexin V-positive cells (AV$^+$) after NK cell coculture with IL2-stimlated CD4$^+$ T cells and M2w. Scale bar; 400 μm. Green; CD4$^+$ cells (CFSE-labeled), red; AV$^+$ cells, yellow; CD4$^+$AV$^+$ double-positive cells.

(C) Gating strategy.

(D) Analysis of dead cells in CD4$^+$CTLA4$^-$ cells. (n = 3)

(E) Analysis of dead cells in CD4$^+$CTLA4$^+$ cells. (n = 4-5)

F-I, Sorted NK cells were tested in an antibody competition assay in coculture with M2w or B78.

(F) Treatment regimen (left) and gating strategy (right).

(G) CD86-positive cells gating and analysis of (H) anti-CD86-PE antibody-bound NK cells and (I) Live$^+$NK cells. (n =2)

(J) Analysis of ULBP MFI in tumor cells. (n = 3)

(K) Analysis of ULBP mRNA expression after recombinant ULBP1 (rULBP1) and NK-κB transcription inhibitor (NK-κBi) stimulation. (n = 4)

(L) Gating strategy (left) and analysis of T_{reg} infiltration. (n = 7-8)

(M) Gating strategy (left) and analysis of T_{em} infiltration. (n = 7-8)

Data represent the mean ± SD. ns, not significant; *P ≤ 0.05; **P ≤ 0.01; ***P ≤ 0.001; ****P ≤ 0.0001.